NON-INVASIVE BLOOD GLUCOSE DETECTION USING AN IMPROVED SPARROW SEARCH ALGORITHM COMBINED WITH AN EXTREME LEARNING MACHINE BASED ON NEAR-INFRARED SPECTROSCOPY[**]

Qing-bo Li[*], Yun-hui Wang

School of Instrumentation and Optoelectronic Engineering, Precision Opto-Mechatronics Technology Key Laboratory of Education Ministry, Beihang University, Beijing, China; e-mail: qbleebuaa@buaa.edu.cn

The traditional way of measuring blood glucose causes pain and inconvenience to patients. Near-infrared spectroscopy is a promising noninvasive alternative. However, the prediction accuracy of the currently used quantitative blood glucose model for near-infrared spectroscopy decreases when a patient's physiological state changes. Therefore, we propose an improved sparrow search algorithm (ISSA) to optimize the initial weights and thresholds of extreme learning machines (ELM) in this paper. We used a tent chaotic map to improve the diversity of the SSA population. We also adopted reverse learning to initialize the population and expand the population search range, which further improved the search performance of the SSA. The predicted results of the ISSA-ELM model were more accurate and generalizable than those of the SSA-ELM model. Clarke error grid analysis showed that the proportion of predicted samples falling into the A region was 90%, and the proportion falling into the B area was 10%, which is in accordance with clinical requirements. Therefore, this model has strong potential for application in non-invasive detection of human blood glucose.

Keywords: *near-infrared spectroscopy, blood glucose detection, chaotic mapping, sparrow search algorithm, extreme learning machine.*

НЕИНВАЗИВНОЕ ОПРЕДЕЛЕНИЕ УРОВНЯ ГЛЮКОЗЫ В КРОВИ С ИСПОЛЬЗОВАНИЕМ УСОВЕРШЕНСТВОВАННОГО АЛГОРИТМА ПОИСКА В СОЧЕТАНИИ С ЭКСТРЕМАЛЬНЫМИ ОБУЧАЮЩИМИ МАШИНАМИ НА ОСНОВЕ СПЕКТРОСКОПИИ В БЛИЖНЕМ ИНФРАКРАСНОМ ДИАПАЗОНЕ

Q. Li [*], Y. Wang

УДК 543.42:547.455.623

Школа приборостроения и оптоэлектроники Бейханского университета, Пекин, Китай; e-mail: qbleebuaa@buaa.edu.cn

(Поступила 23 февраля 2022)

Для неинвазивного определения уровня глюкозы в крови человека предложен усовершенствованный алгоритм поиска (ISSA) с целью оптимизации начальных весов и порогов машин экстремального обучения (ELM). Карта палаточного хаоса использована для улучшения разнообразия SSA, обратное обучение — для инициализации популяции и расширения диапазона поиска популяции, что повышает производительность SSA. Результаты модели ISSA-ELM являются более точными и обобщающими по сравнению с моделью SSA-ELM. Анализ сетки ошибок Кларка показывает, что доля предсказанных образцов, попадающих в область А, составляет 90 %, в область В — 10 %, что соответствует клиническим требованиям.

Ключевые слова: *спектроскопия в ближнем инфракрасном диапазоне, определение уровня глюкозы в крови, хаотическое картирование, алгоритм поиска, машина с экстремальным обучением.*

[**] Full text is published in JAS V. 90, No. 3 (http://springer.com/journal/10812) and in electronic version of ZhPS V. 90, No. 3 (http://www.elibrary.ru/title_about.asp?id=7318; sales@elibrary.ru).

Introduction. Diabetes is a metabolic disorder caused by genetics, immune dysfunction and other factors. When patients are in a state of hyperglycemia for a long time, serious complications can occur, such as retinopathy, cardiovascular disease and nephropathy. According to the International Diabetes Federation, approximately 537 million adults worldwide were expected to suffer from diabetes in 2021, with the incidence increasing year by year [1]. Currently, diabetes cannot be cured and requires lifelong management through control of blood glucose, which is achieved by insulin injection and other means. The composition of human blood is complex and blood glucose concentration is relatively low. Moreover, prediction becomes difficult when a person's physiological state changes. Therefore, it is important to obtain accurate blood glucose information quickly and, ideally, noninvasively [2, 3].

The theoretical basis of infrared spectroscopy is described by the Beer–Lambert law [4, 5]. The near-infrared spectral region covers the sum frequency and double frequency absorption regions of hydrogen-containing groups, such as hydroxyl (O–H) and methyl (C–H) groups of glucose, which can be used to quantify the glucose concentration [6]. Non-invasive detection of blood glucose can be realized using chemometric analysis technology to establish a mathematical model of spectral data and the blood glucose concentration [7]. The Sandia National Laboratory of the United States and the University of New Mexico School of Medicine [8] cooperated in a series of blood glucose detection studies using near-infrared spectroscopy. This demonstrated the potential of NIR spectroscopy in the field of non-invasive blood glucose detection for the first time. Carlos and Benhard [9] noted that the absorption of water at the near-infrared wavelengths of 1212–1850 and 2120–2380 nm is low, but the measurement signal has high energy. Li and Huang [10] greatly improved the prediction accuracy by establishing a quantitative model of human blood glucose by performing net signal preprocessing on near-infrared spectral data combined with radial basis partial least squares regression.

Extreme learning machines (ELM) is a single hidden layer feedforward neural network proposed by Huang et al. [11]. ELM has better robustness and higher convergence speed than a traditional neural network. However, because the input weights and hidden layer thresholds of ELM are randomly selected, the stability and robustness of the model need to be further improved. On this basis, we established an improved sparrow search algorithm (ISSA) to optimize the ELM (hereafter, the ISSA-ELM model). This model achieved fast and continuous non-invasive blood glucose detection within the clinically allowable error range.

Experiment. The spectrometer was a NIRquest256-2.5 near-infrared miniature spectrometer produced by Ocean Optics (USA). The effective wavelength range was 850–2500 nm, the spectral resolution was 9.5 nm, the integration time was 28 ms, the spectrum scanning time was 20, and the smoothness was 5-point. The light source (HL-2000-HP) and optical fiber (R400-7-VIS-NIR Y-type) were supplied by Ocean Optics. A Verio Flex blood glucose meter (Onetouch Medical Co., USA) was used, which had a detection range of 1.1–33.3 mmol/L.

The subjects were two healthy volunteers, referred to as volunteer A and volunteer B. To verify the generalization performance of the model, three data-acquisition experiments were performed on different days for each volunteer. The volunteers fasted for 12 h before the experiment and ingested 300 mL of 0.25 g/mL aqueous glucose solution during the experiment. The fingertip spectral data of the volunteers were collected with the spectrometer, and the blood glucose concentration was measured with the glucose meter. The collection interval was 5–7 min. Measurements were stopped on the first day when the volunteers' blood glucose concentrations returned to those of their fasting state. On days 2 and 3, Measurements were stopped when the volunteers' blood glucose concentrations reached those of their peak state. We note that volunteers should remain calm and not undertake strenuous exercise when collecting data. Volunteer A received 18, 10, and 10 samples on days 1, 2 and 3, respectively, during which their blood glucose concentration varied from 5.4 to 11.1 mmol/L. Volunteer B received 15, 7, and 7 samples on days 1, 2, and 3, respectively, during which their blood glucose concentration ranged from 5.2 to 9.7 mmol/L.

The spectral data were first preprocessed using multivariate scattering correction to eliminate the spectral differences caused by different scattering levels. This enhanced the correlation between the spectrum and the substance to be measured [12].

As mentioned previously, we used an ISSA to optimize the initial weights and thresholds of the ELM [13]. By introducing tent mapping, the randomness and ergodicity of chaotic sequences could be used to improve the diversity of the population. The inverse solution generated by the reverse-learning strategy was used to expand the search range of the population and improve the search performance of the algorithm. The overall modeling steps are as follows:

Step 1. The parameters are initialized, such as the population size, maximum number of iterations, producer ratio (PD), the ratio of those who perceive danger to those who do not (SD), and safety threshold (ST).

Step 2. The upper and lower boundaries of the optimization variables are determined. Tent mapping and the reverse-learning strategy are then used to generate the initial sparrow population [14]. The tent-mapping formula is as follows:

$$X_{k+1} = \begin{cases} 2X_k, 0 \le X_k \le 0.5, \\ 2(1 - X_k), 0.5 < X_k \le 1. \end{cases} \tag{1}$$

The tent-mapping equation generates N solutions X_i (i = 1, 2, …, N) as the initial population, and the reverse solutions, X_i^*, are generated for each initial solution:

$$X_i^* = X_{\min} + X_{\max} - X_i \tag{2}$$

where $X_{\min}$ and $X_{\max}$ represent the minimum and maximum values of the initial solution, respectively. Finally, the initial solution and the reverse solution are merged, and N individuals with better fitness are selected to form the initial population [15].

Step 3. The adaptive value is calculated for each sparrow. The optimal fitness value and the worst fitness value are determined, and their positions are recorded.

Step 4. From the sparrows with the best fitness values, some are selected as producers to update their positions. The producer can search for food in a wide range of places. The location of the producer is updated as described below during each iteration:

$$X_{i,j}^{t+1} = \begin{cases} X_{i,j}^t \cdot \exp\left(-\dfrac{i}{a \cdot \text{iter}_{\max}}\right), R_2 < ST \\ X_{i,j}^t + Q \cdot L, R_2 \ge ST \end{cases} \tag{3}$$

where t is the number of iterations, $X_{i,j}$ is the position information of the ith sparrow population in the jth dimension, a is a random number (a∈(0,1)), $\text{iter}_{\max}$ is the maximum number of iterations, Q is a normal distribution random number (Q∈[0,1]), L shows a matrix of 1×d for which each element inside is 1, R_2 is the alarm value (R_2∈[0,1]), and ST is the safety threshold (ST∈[0.5,1]). When $R_2 < ST$, there are no predators in the foraging environment, and the producer can conduct extensive search operations. If $R_2 \ge ST$, some sparrows in the population have discovered predators, an early warning is issued to other sparrows in the population, and all sparrows need to fly to a safe area for foraging.

Step 5. During the foraging process, other sparrows named scroungers monitor the producer. When the producer finds better food, the scrounger will compete with the producer. If successful, the scrounger will get the producer's food; otherwise, they will continue to track and monitor producer. The location of the scrounger is updated as described below during each iteration:

$$X_{i,j}^{t+1} = \begin{cases} Q \exp\left[\left(X_{\text{worst}}^t - X_{i,j}^t\right) \Big/ i^2\right], & i > N/2, \\ X_P^{t+1} + \left|X_{i,j}^t - X_P^{t+1}\right| A^+ L, & i \le N/2, \end{cases} \tag{4}$$

where X_{worst} is the global worst position. X_P is the optimal position occupied by the producer, A is a 1×d matrix of 1 or –1 randomly assigned to each element, and $A^+ = A^T(AA^T)^{-1}$. When $i > N/2$, the i^{th} scrounger with poor fitness has not obtained food and needs to go to other areas to find food.

Step 6. Some sparrows are selected from the population as alerters whose positions are randomly generated. The mathematical model can be expressed as follows:

$$X_{i,j}^{t+1} = \begin{cases} X_{\text{best}}^t + \beta \left|X_{i,j}^t - X_{\text{best}}^t\right|, f_i > f_g, \\ X_{i,j}^t + k \dfrac{\left|X_{i,j}^t - X_{\text{worst}}^t\right|}{f_i - f_w + \varepsilon}, f_i = f_g, \end{cases} \tag{5}$$

where X_{best} is the global best position; β is the step-size adjustment coefficient of a randomly generated normal distribution with mean of 0 and a variance of 1; k is a uniform random number in the range of [0,1], indicating the sparrow movement direction; f_g and f_w are the global optimal and worst fitness values; f_i is the fitness value of the present sparrow; and ε is the minimum constant to prevent the denominator from being 0. When $f_i > f_q$, the sparrow is at the edge of the population and can be easily attacked by natural ene-

mies; when $f_i = f_q$, the sparrow in the center of the population is informed of the danger of being attacked by enemies and needs to move closer to the other sparrows [16].

Step 7. Determine whether the maximum number of iterations is reached. If so, the iteration is stopped and the training parameters are saved. The optimal results, X_{best} and f_g, are input into the ELM. The output weights are calculated, and the complete model is established.

Results and discussion. The spectra taken for each volunteer on days 1 and 2 were used as the calibration set to establish the ISSA-ELM model, and the spectra taken on day 3 were used as the test set to evaluate the accuracy of the model. For volunteer A, 28 spectra were use in the calibration set and 10 were used in the test set. For volunteer B, 22 spectra were used in the calibration set and 7 were used in the test set. The predicted results based on the calibration set and test set are shown in Figs. 1, and Table 1.

Figures 1 show that the ISSA-ELM method accurately predicted results for both calibration and test sets. For volunteer A (Fig. 1A), the relative errors (except for sample 8) were all less than 20%, while for volunteer B (Fig. 1B), the relative errors (except for sample 7) were all less than 20%. There was a strong correlation between the blood glucose concentration and the spectral data.

Compared with the SSA-ELM model, the root mean square error of prediction (RMSEP) values of the ISSA-ELM model for volunteers A and B was reduced by 0.41 and 0.5 mmol/L, respectively. The correlation coefficient (R) increased by 0.18 and 0.07, respectively. The residual predictive deviations (RPDs) [17, 18] of the ISSA-ELM prediction model for volunteers A and B were both greater than 1.4, which were 0.5 and 0.51 better than those of the SSA-ELM prediction model.

To further verify the effectiveness of the ISSA-ELM model, the Clarke Error Network [19] was used to evaluate the experimental results, which are shown in Fig. 2 and Table 2.

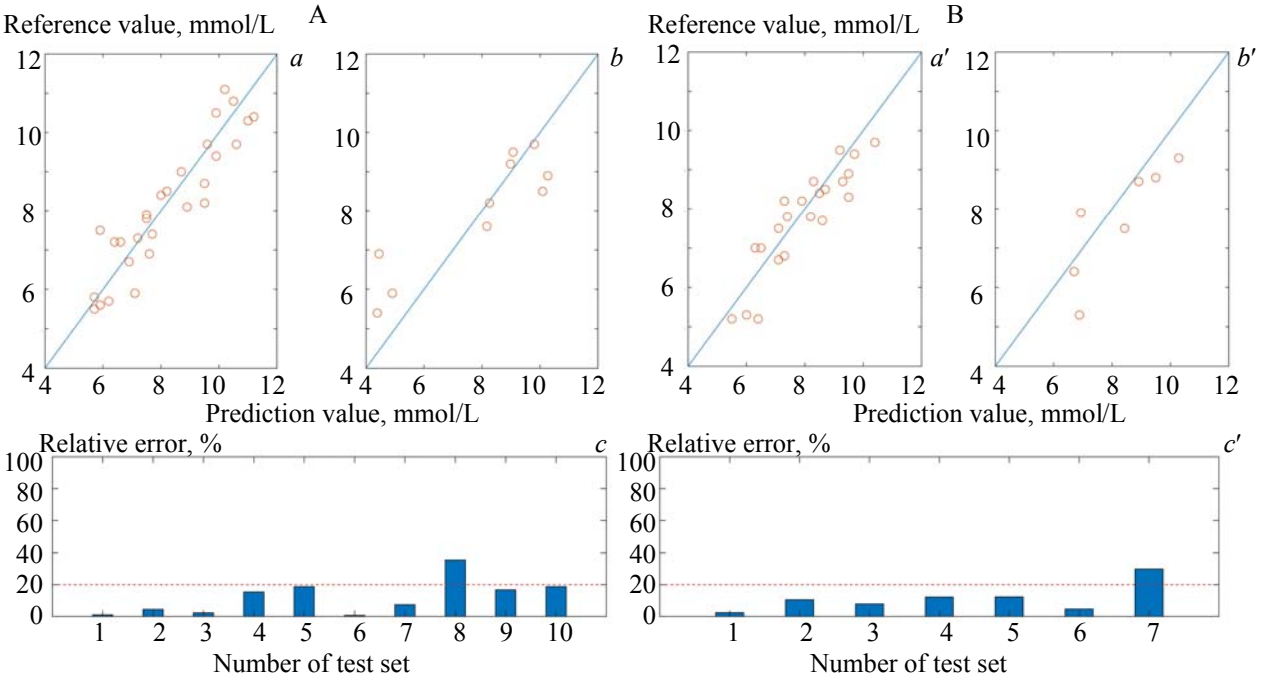

Fig. 1. Predicted results from the ISSA-ELM model for volunteers A and B: Reference and predicted values for relative error the calibration (a, a′), reference and predicted values for the test (b, b′), and relative error of the test (c, c′).

TABLE 1. Performance Comparison of the Two Models

Volunteer	Model	Calibration set				Test set		
		RMSECV	R	RPD		RMSEP	R	RPD
A	SSA-ELM	0.82	0.88	2.1		1.54	0.72	1.37
	ISSA-ELM	0.68	0.92	2.6		1.13	0.90	1.87
B	SSA-ELM	0.85	0.83	1.6		1.42	0.77	1.42
	ISSA-ELM	0.62	0.89	2.3		0.92	0.84	1.91

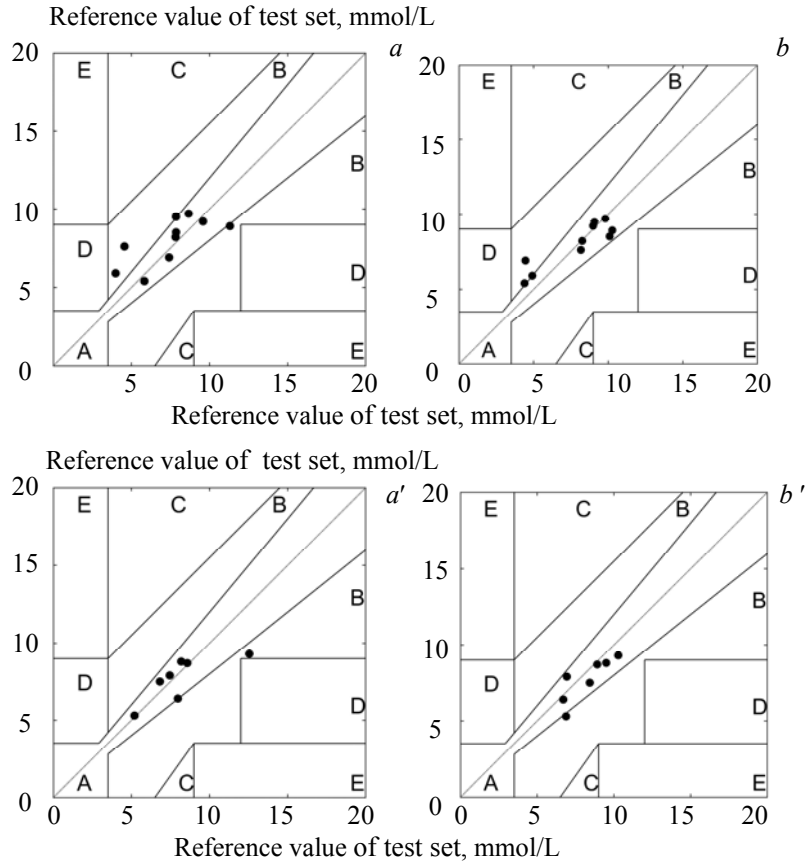

Fig. 2. Clarke results for volunteer A and B: SSA-ELM model (a, a′), and ISSA-ELM model (b, b′).

TABLE 2. Clarke Error Grid Analysis for the Two Models

Volunteer	Model	Clarke error grid analysis, %				
		A	*B*	*C*	*D*	*E*
A	SSA-ELM	70	30	0	0	0
	ISSA-ELM	90	10	0	0	0
B	SSA-ELM	80	20	0	0	0
	ISSA-ELM	90	10	0	0	0

Clarke's error grid analysis of the ISSA-ELM model for volunteers A and B showed that 90% of the samples fell in area *A* and 10% fell in area *B*, indicating that the model had good reliability. Thus, the ISSA not only improved the population diversity and search range, but also it had a stronger search ability than SSA. Moreover, the ISSA-ELM model solved the complex nonlinear relationship between the spectral data and blood glucose concentration and avoided falling into a local optimum.

For the calibration set, which was composed of data from the first and second days of the experiment, the RMSECV of the ISSA-ELM was less than 0.7 mmol/L, indicating good prediction accuracy. When the data from the first and second days were used for modeling, and the third day's data were used as the test set, the physiological state of the volunteers (such as body temperature), parameters of the spectrometer (for example, owing to instability of the light source) and measurement conditions (such as ambient temperature and humidity) would have changed, which made the prediction more difficult. The RMSEP values for both volunteers were less than 1.2 mmol/L. Thus, the ISSA-ELM model has good adaptability and robustness, making it suitable for more complex application scenarios of blood glucose detection.

Conclusions. We proposed an improvement of the sparrow search algorithm by introducing chaotic mapping and reverse learning to initialize its population. This algorithm was used to optimize an extreme learning machine thereby establishing an ISSA-ELM prediction model. We used the model to predict the concentrations of blood glucose in two volunteers. The RMSEP values were 1.13 and 0.92 mmol/L, respectively, which verified the effectiveness and robustness of the model, and its potential for application in non-invasive blood glucose detection methods in humans.

REFERENCES

1. The Tenth Edition of the IDF Diabetes Atlas, International Diabetes Federation (2021).
2. S. Guo, H. Su, X. C. Huang, *Chin. Optics*, **12**, 1235–1248 (2019).
3. F. M. Stephen, L. R. Timothy, B. B. Thomas, *Clin. Chem*., **45**, 1651–1658 (1999).
4. K. Sumaporn, Y. P. Du, *Chemometrics and Intell. Lab. Systems*, **82**, 97–103 (2006).
5. D. W. Zhang, G. Zhao, R. J. Hong, *Opt. Instrum.*, **39**, 87–94 (2017).
6. X. D. Chen, J. Gao, H. Q. Ding, *Chin. Optics*, **5**, 317–326 (2012).
7. K. V. Sandeep, *Anal. Chim. Acta*, **750**, 16–27 (2012).
8. M. R. Robinson, R. P. Eaton, D. M. Haaland, *Clin. Chem*., **38**, 1618–1622 (1992).
9. E. F. Carlos, W. Benhard, *Med. Eng. Phys*., **30**, 541–549 (2008).
10. Q. B. Li, G. W. Huang, *Spectrosc. and Spectr. Analysis*, **34**, 494–497 (2014).
11. G. B. Huang, H. M. Zhou, X. J. Ding, R. Zhang, *IEEE Trans. Syst. Man Cybern. B: Cybern*, **42**, 513–529 (2012).
12. C. A. Engelbrecht, *Nuclear Instruments and Methods*, **93**, 103–107 (1971).
13. J. K. Xue, B. Shen, *Systems Science & Control Engineering*, **8**, 22–34 (2020).
14. Y. M. Fang, X. D. Zhao, P. Zhang, *Control Theory & Applications*, **37**, 1644–1654 (2020).
15. X. W. Xia, J. N. Liu, Y. X. Li, *J. Software*, **9**, 350–357 (2014).
16. Q. H. Mao, Q. Zhang, *J. Frontiers of Computer Science and Technology*, **15**, 1155–1164 (2021).
17. T. Fearn, *NIR News*, **13**, 12–14 (2002).
18. P. C. Williams, *American Association of Cereal Chemists*, St Paul, MN, USA, 164 (2001).
19. W. L. Clarke, D. Cox, L. A. Gonderfrederick, *Diabetes Care*, **23**, 622–628 (1987).